Available online at www.sciencedirect.com
SCIENCE DIRECT®
Journal of Crystal Growth 272 (2004) 719–725
JOURNAL OF CRYSTAL GROWTH
www.elsevier.com/locate/jcrysgro

Characteristics of InGaAsN/GaAsN quantum well lasers emitting in the 1.4-μm regime

Jeng-Ya Yeh[a,*], Luke J. Mawst[a], Nelson Tansu[b]

[a]*Department of Electrical and Computer Engineering, Reed Center for Photonics, University of Wisconsin-Madison, 1415 Engineering Drive, Madison, Wisconsin 53706, USA*
[b]*Department of Electrical and Computer Engineering, Center for Optical Technologies, Lehigh University*

Abstract

To improve the performance of metalorganic chemical vapor deposition (MOCVD)-grown long wavelength InGaAsN quantum well (QW) diode lasers emitting beyond 1.3 μm, a detailed examination of the growth parameters was performed, including DMHy/V ratio, QW growth temperature, choice of barrier material and thermal annealing temperature. This study reveals that a growth temperature in the 530–540 °C range is preferred in order to improve nitrogen incorporation and prevent degradation of the material luminescence. Increasing the DMHy/V ratio is found to be the preferred method to achieve wavelength extension. Utilization of GaAsN barrier layers, instead of GaAs barriers, suppresses the spectral blue-shift of the quantum well luminescence after thermal annealing treatment. Under optimized growth conditions, InGaAsN diode lasers emitting at 1.378 μm are realized with a threshold current density of 661 A/cm^2 and external differential quantum efficiency of 34%. Lasing wavelengths as long as 1.41 μm with a threshold current density of 1.93 kA/cm^2 are also demonstrated, representing the longest wavelength InGaAsN QW lasers realized by MOCVD.

PACS: 42.55.P, 81.40.E, 78.66, 81.15.G, 61.10.N, 78.55.E

Keywords: A1. Thermal annealing; A1. X-ray diffraction; A3. Metalorganic chemical vapor deposition; B2. GaAsN; B2. InGaAsN; B3. Long wavelength quantum well laser

1. Introduction

Proposed by Kondow et al., InGaAsN opens up new opportunities to realize low-cost, high-performance 1.3-μm emitting semiconductor diode lasers grown on GaAs substrates. With intensive research effort, high-performance 1.3-μm emitting

*Corresponding author. Tel.: +1-608-265-5403; fax: +1-608-265-4623.
E-mail address: jyeh@cae.wisc.edu (J-Y. Yeh).

0022-0248/$ - see front matter © 2004 Elsevier B.V. All rights reserved.
doi:10.1016/j.jcrysgro.2004.09.005

InGaAsN quantum well (QW) lasers have been successfully demonstrated and optimized by both molecular beam epitaxy (MBE) [1,2] and metalorganic chemical vapor deposition MOCVD growth [3–7]. Optimized structures exhibit reduced threshold current density and lower temperature sensitivity as compared to conventional InP-based 1.3-μm emitting lasers [8,9]. One challenging goal remaining is to extend the emission wavelength beyond 1.3 μm, while maintaining optical material quality for the realization of longer wavelength, high-performance, GaAs-based devices. Dilute-nitride material grown by MBE has shown promising characteristics in the 1.4–1.5-μm wavelength regime. Gollub et al. demonstrated 1.49-μm emitting ridge waveguide lasers with a threshold current of 120 mA and maximum power of 15 mW [10]. Recently, by introducing antimony into the InGaAsN QW, Bank et al. demonstrated 1.49-μm emitting devices with threshold current densities as low as 1.1 kA/cm^2 and external differential quantum efficiencies of 34% [11]. While these results are promising, they do not yet match the device performance of conventional InP-based lasers in the 1.5 μm-wavelength region.

For MOCVD growth, the emission wavelength and material quality of the InGaAsN QW is limited by the imperfection of the nitrogen precursor and the competing behavior of indium and nitrogen incorporation. Up to now, the longest lasing wavelength of MOCVD-grown InGaAsN devices has been limited to 1.38 μm with a relatively high threshold current density of 2.2 kA/cm^2 [5]. In order to fully explore the possibilities of wavelength extension, it is essential to study the effects of the various MOCVD growth conditions on the InGaAsN material properties and the resulting device behavior. Typically, wavelength extension comes at the expense of material quality degradation due to an increased N-content in the QW. In this work, a systematic investigation was conducted on *gas-phase DMHy/V ratio, QW growth temperature and thermal annealing temperature*.

In addition, the *choice of the material system for the barrier* surrounding the QW is also important to the device performance. Previous work identified that substituting GaAs barriers with tensile strained $GaAs_{1-x}P_x$ ($x\sim0.15$ and 0.33) effectively suppresses carrier leakage, leading to lower device temperature sensitivity. The temperature sensitivity of the threshold current density (J_{th}) and external differential quantum efficiency (η_d) are characterized by T_0 and T_1 values, respectively ($T_0 = 1/J_{th} \times (\partial J_{th}/\partial T)$, $T_1 = -1/\eta_d(\partial\eta_d/\partial T)$). The T_1 value of InGaAsN–$GaAs_{0.67}P_{0.33}$ lasers (2 mm-long cavity) is 450 K, significantly improved compared with values of 160 K for the lasers with GaAs barriers [12]. However, utilization of a high bandgap material as the barrier inevitably incurs a stronger quantum confinement effect and emission wavelength blue-shift. This motivates the idea of employing smaller bandgap material (such as GaAsN) for the purpose of realizing longer wavelength lasing devices, at the possible expense of reduced carrier confinement. Previously, we demonstrated 1317-nm emitting InGaAsN–GaAsN lasers with improved threshold current density and T_0 compared to GaAs barrier structures [13]. Other reports, using MBE grown material, by Egorov et al. also demonstrated improved threshold current, but degraded T_0 values for their single QW InGaAsN–GaAsN lasers [14].

2. Experimental procedure

The structures studied were grown on (1 0 0) n-GaAs substrate with group III sources of trimethylgallium (TMGa), trimethylaluminum (TMAl) and trimethylindium (TMIn), and group V material sources of AsH_3, PH_3 and U-dimethylhydrazine (U-DMHy). The highly compressive-strained 6-nm $In_{0.4}Ga_{0.6}As_{1-x}N_x$ QW was grown at a reactor pressure of 200 mbar with a QW growth rate of approximately 1.28 μm/h. The approximate total hydrogen flow rate was 5200 sccm. Each structure was completed in a single growth step (i.e. no regrowth).

In this work, we focus on two variations of the $In_{0.4}Ga_{0.6}As_{1-x}N_x$ QW active region (~2.7% compressive strain). The first consists of 75-Å $GaAs_{0.85}P_{0.15}$ tensile-strained layers, employed for strain compensation, with 100-Å GaAs bounding layers on both sides of the InGaAsN QW, as

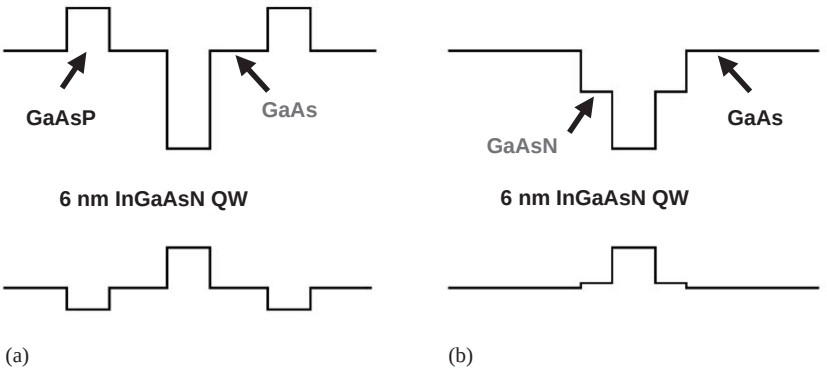

Fig. 1. Schematic band diagram of InGaAsN QW with (a) GaAs and (b) GaAsN barrier. Tensile-strained GaAsP barriers in structure (a) provides strain compensation.

shown in Fig. 1(a). In the second structure, shown in Fig. 1(b), the direct barrier was replaced with 35-Å $GaAs_{1-y}N_y$ where the N-content y was varied to be 0%, 1.5% and 2.5%. The separate confinement heterostructure (SCH) consists of a 300-nm undoped GaAs with 0.1-μm thick $Al_{0.75}Ga_{0.25}As$ cladding layers.

Room temperature (300 K) and low temperature (25 K) photoluminescence (PL) measurements were conducted to characterize the material luminescence properties and the excitation source was an argon ion laser ($\lambda = 500$ nm). High-resolution X-ray diffraction (XRD) experiments were also carried out to determine the material composition and investigate the effect of thermal annealing on the InGaAsN–GaAs and InGaAsN–GaAsN interface quality.

3. Results and discussion of MOCVD growth studies

3.1. Effects of QW growth temperature and gas-phase DMHy/V ratio

By altering the ratio of AsH_3 to DMHy flow rates, one can finely tune the material composition to the desired emission wavelength target [15]. Here, we assigned the ratio of gas-phase DMHy flow to total group V material flow, DMHy/V, as a growth variable and study its effect on the InGaAsN QW luminescence property. In our experiment, we fixed DMHy flow at 5.12×10^{-3} mol/min and modified AsH_3 flow, keeping the V/III ratio around 230. The AsH_3 flow was varied from 4.46×10^{-4} to 8.57×10^{-5} mol/min, corresponding to a DMHy/V ratio from 0.969 to 0.994. In this study, structures shown in Fig. 1(a) and a short thermal annealing treatment (640 °C) of 3 min were used.

Fig. 2(a) shows the measured room temperature PL spectral peak wavelength and intensity as functions of DMHy/V. With increasing DMHy/V, the emission wavelength increases from 1220 nm with a ratio of 0.969 to emission wavelengths of 1450 nm with a ratio of 0.994, indicating that the emission wavelength of InGaAsN QW is very sensitive to the DMHy/V ratio. Without introducing DMHy, a 6-nm $In_{0.4}Ga_{0.6}As$ QW emits at 1.22–1.23 μm, which is approximately equal to the wavelength of InGaAsN QW with DMHy/V = 0.969. Therefore, significant nitrogen incorporated into the QW occurs only when the DMHy/V ratio reaches values above 0.969. With a small change of DMHy/V, the wavelength can be engineered over a wide range from 1.2 to 1.5 μm. When the wavelength is extended from 1220 to 1450 nm, the PL intensity drops about 20 times and the spectral full-width at half-maximum (FWHM) slightly increases from 59.5 to 62.4 meV, indicating a degrading material quality as the N-content increases.

The growth temperature of the InGaAsN QW is also crucial to material optimization [16,17].

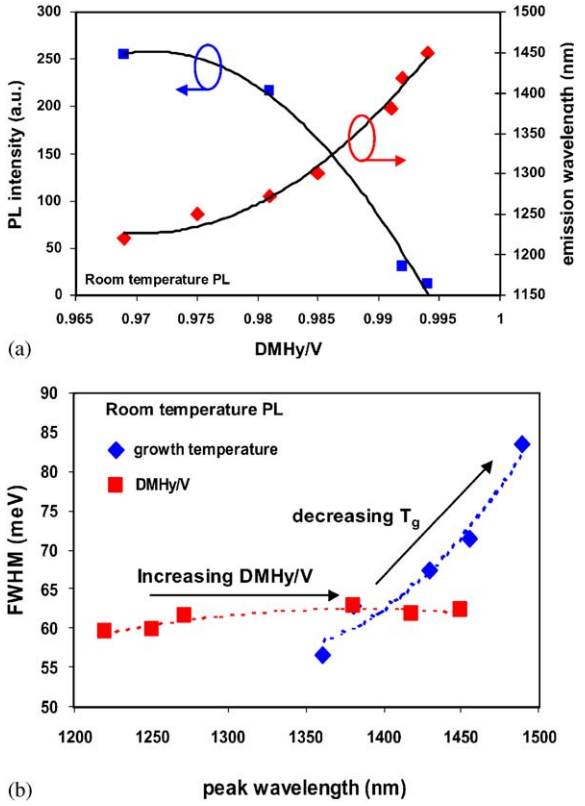

Fig. 2. (a) Room temperature PL spectrum peak intensity and emission wavelength as functions of gas-phase DMHy/V ratio for the InGaAsN/GaAs structure. (b) PL spectrum FWHM of the InGaAsN–GaAs QW structure with varying growth temperature or DMHy/V ratio. A large spectral broadening was observed when reducing the InGaAsN growth temperature.

Reducing the growth temperature can significantly increase N-incorporation efficiency which results in wavelength extension as well as deterioration of crystalline structure. In this experiment, a QW growth temperature ranging from 490 to 540 °C was utilized and DMHy/V ratio was fixed at 0.991. Generally, reducing growth temperature by 10 °C leads to a wavelength red-shift of 20–30 nm. At a low temperature of 490 °C, one is able to achieve emission wavelengths as long as 1500 nm. However, large spectral broadening suggests that a lower growth temperature is not the solution for realizing high-performance InGaAsN QW lasers emitting around 1.5 μm. The increase of FWHM is possibly due to alloy cluster scattering. Generally, compositional phase separation from immiscibility is more severe at a lower growth temperature. The dependence of the PL FWHM vs. emission wavelength is shown in Fig. 2(b) with two series of data, indicating the effects of QW growth temperature and DMHy/V. Interestingly, unlike varying the growth temperature, the FWHM values remains similar (60–63 meV) with increasing DMHy/V. The study shows that utilizing a growth temperature around 530–540 °C while varying DMHy/V ratio represents a more practical and optimal growth method for achieving long wavelength InGaAsN lasers beyond 1.4 μm.

3.2. GaAsN barrier QW structure

GaAsN can serve as an alternative material to surround the InGaAsN QW, as shown in Fig. 1(b) [10,18]. Thorough investigations of the use of GaAsN barriers were carried out using MBE growth techniques [10,18], while few MOCVD studies have been reported [13]. GaAsN with smaller bandgap energy and tensile-strain reduces the quantum size effect so that emission wavelength elongation of the InGaAsN–GaAsN QW compared to InGaAsN–GaAs can be realized, and secondly, it provides strain compensation for the highly compressive-strained InGaAsN QW (−2.7%) and therefore enhances the material quality.

Various N-contents of 0%, 1.5% and 2.5% in the GaAsN barrier were used to examine the effect on the InGaAsN QW. All the samples were annealed at 720 °C for 27 min to improve the optical quality. It is important to note that without this high-temperature annealing process, the InGaAsN–GaAsN QW shows very poor PL intensity. A detailed study of the in-situ thermal annealing effect is presented in Section 3.3.

With $GaAs_{0.985}N_{0.015}$ barriers, the peak wavelength of the $In_{0.4}Ga_{0.6}As_{0.9915}N_{0.0085}$ QW exhibits a red-shift of about 35 nm while the PL intensity drops by one-half compared to the structure with identical QW except GaAs barrier. This indicates that there is no significant material degradation when utilizing a N-containing barrier and the GaAsN barrier is suitable for long wavelength

InGaAsN QW lasers emitting beyond 1.3 μm. Comparing the emission wavelengths of structures with $GaAs_{0.985}N_{0.015}$ and $GaAs_{0.975}N_{0.025}$ barriers, we find that no further wavelength extension is achieved with increasing barrier N-content. The FWHM of the PL spectrum of each sample was measured to be near 35 meV with negligible variation.

3.3. InGaAsN–GaAs(N) thermal annealing studies

Thermal annealing is well known for improving the InGaAsN material quality with an expense of an undesirable wavelength blue-shift. The influence on emission wavelength is possibly due to changes of nitrogen atom nearest-neighbor configuration [19–22], or atomic interdiffusion [20,23,24]. For growing high-quality InGaAsN QWs, thermal annealing is a necessary treatment to enhance the material luminescence property. Here, we focus on the investigation of InGaAsN–GaAs(N) QW structures under various annealing condition.

Figs. 3(a) and (b) show the low-temperature PL peak intensity and emission wavelength of the InGaAsN–GaAs and InGaAsN–$GaAs_{0.985}N_{0.015}$ QWs annealed in the range 640–720 °C. The QW contains 40% In and 0.85% N, an exhibiting emission wavelength at 1380 nm with GaAs barriers at room temperature. We found that the choice of barrier material also influences the effect of thermal annealing. An InGaAsN QW with either GaAs or GaAsN barrier both show enhanced PL intensity after annealing at high temperature. However, the intensity of the InGaAsN–GaAsN structure tends to saturate, a behavior not observed for the samples with GaAs barrier. The PL spectrum FWHM of the GaAs-barrier structures are 31.8, 32.3, 36.9, 40.8 meV after annealing at 700, 680, 660 and 640 °C. For GaAsN-barrier samples, FWHM was also *improved from* 66 *to* 37 *meV* for 640 and 720 °C annealing, respectively. This dramatic improvement in the PL FWHM values demonstrates the importance of annealing treatment for N-containing barrier structures.

Another distinction between these two structures is the annealing-induced wavelength blue-shift shown in Fig. 3(b). A more substantial blue-shift, as large as 54–87 nm, was observed for the GaAs-barrier structure while only a 20–64 nm blue-shift occurs when $GaAs_{0.985}N_{0.015}$ is utilized (640 °C annealed sample as a reference). The suppression of the wavelength blue-shift of annealed InGaAsN–GaAsN QWs was also reported by the MBE-grown materials [22,25]. To examine the effect of thermal annealing on the QW–barrier interface, high-resolution XRD experiments were conducted on the InGaAsN–GaAs(N) superlattice (SL) structures. The four-period SL samples consist of 6-nm $In_{0.4}Ga_{0.6}As_{0.995}N_{0.005}$ QW surrounded by 12-nm GaAs or $GaAs_{0.985}N_{0.015}$ barriers and annealed at 700 °C for 27 min after the growth of SL structures. Comparing the as-grown and annealed samples, the FWHM and peak-to-valley ratio of the satellite peaks are almost identical which indicates no significant structural degradation of the interfacial sharpness.

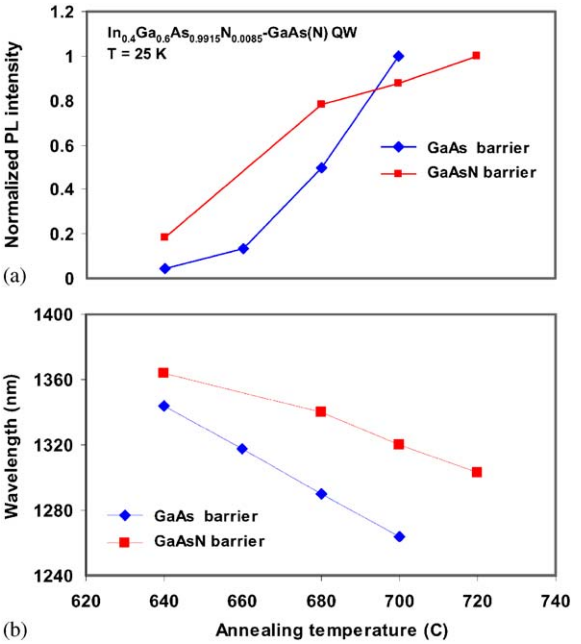

Fig. 3. Low-temperature (a) PL intensity and (b) emission wavelength of the InGaAsN QW with GaAs or GaAsN barrier treated at various annealing temperatures. A reduced blue-shift was observed for the samples with GaAsN barrier.

4. InGaAsN–GaAsN QW lasers emitting at $\lambda > 1.3\,\mu m$

Based on the MOCVD growth optimization of the InGaAsN QW, we are able to achieve InGaAsN QW lasers beyond 1.3 μm with improved device characteristics. Here, the approach we take is to utilize a higher DMHy/V ratio and GaAsN barriers to extend the emission wavelength along with higher annealing temperatures to improve the material quality. Two laser structures emitting in the 1.4-μm regime have been fabricated and carefully characterized. Both the lasers consist of $GaAs_{0.985}N_{0.015}$ barriers around an $In_{0.4}Ga_{0.6}As_{1-x}N_x$ QW with DMHy/V ratio of 0.991 for 1.378-μm emitting laser (laser A) and 0.994 for 1.41-μm emitting laser (laser B). We estimate the N-content of the QW to be around 0.85% and 0.9%, respectively, based on extrapolation from 1.3-μm emitting structures. The thermal annealing process was completed during the growth of the 1.1-μm p-type AlGaAs cladding layer. For laser A, the annealing temperature was 680 °C and increased to 700 °C for laser B. Other growth conditions and the laser structure were identical for these two bases. The growth temperature of the 6-nm InGaAsN QW was fixed at 530 °C and the reactor pressure was 200 mbar. The 300-nm undoped GaAs separate confinement heterostructure (SCH) and 1.1-μm bottom AlGaAs cladding layers ($n \sim 10^{18}\,cm^{-3}$) were grown at 530 and 775 °C, respectively. Broad area lasers with a stripe width of 100 μm, defined by V-groove etching and 1000-Å SiO_2 passivation, were fabricated and characterized.

In Fig. 4, the light power vs. injection current (*L–I*) curve at 20 °C of lasers A and B under pulsed operation (1% duty cycle) are shown. A very low J_{th} of only 661 A/cm^2 and lasing wavelength of 1378 nm for 800-μm long devices were obtained. The external differential quantum efficiency was measured to be 34% for the as-cleaved devices. For 1-mm long devices, J_{th} and η_d of the 1379-nm emitting lasers are 563 A/cm^2 and 25.4%, respectively, representing the highest performance of InGaAsN QW lasers achieved by MOCVD near the 1400-nm wavelength region. The temperature sensitivity of device characteristics was also

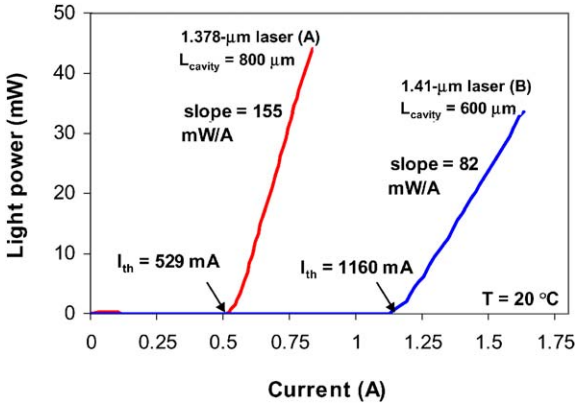

Fig. 4. Light power vs. current (*L–I*) relation of the 1.378-μm (laser A) and 1.41-μm (laser B) InGaAsN–GaAsN QW lasers.

measured. From 20 to 60 °C, the threshold current increases with a T_0 value of 67 K and the differential quantum efficiency decreases with a T_1 value of 70 K for 800-μm long devices. A significant improvement of laser performance is achieved compared to our previous results of 1380-nm lasers [26]. The previous laser structure consisted of an $In_{0.4}Ga_{0.6}As_{0.9915}N_{0.0085}$ QW with GaAs barriers, subjected to an annealing temperature of 640 °C. J_{th} and η_d values were 1010 A/cm^2 and 27%, respectively, and characteristic temperatures T_0 and T_1 of 73 and 55 K were quantified. The slight increase of T_1 from 55 to 70 K suggests that losing carrier confinement from using GaAsN barrier structures does not necessarily lead to stronger temperature sensitivity. By employing the optimal growth conditions and device structure established here, we were able to successfully reduce J_{th} by 45% and enhance η_d by about 25%. This improvement in device performance demonstrates the benefit of utilizing a higher thermal annealing temperature in combination with a GaAsN barrier. For the 1.41-μm laser (B), J_{th} and η_d were measured to be 1.93 A/cm^2 and 19% for the uncoated 600-μm devices. The degradation of laser performance at 1.41 μm probably results from the higher QW N-content leading to increased monomolecular (nonradiative) recombination. Nevertheless, this data represent the *longest wavelength* InGaAsN QW lasers achieved to date by MOCVD.

5. Summary

In the effort to improve the performance of long wavelength InGaAsN quantum well (QW) diode lasers emitting beyond 1.3 μm grown by MOCVD, a detailed examination of the growth parameters was performed, including *DMHy/V ratio, QW growth temperature, choice of barrier material and thermal annealing temperature*. This study identifies that a growth temperature in the 530–540 °C range is preferred in order to improve nitrogen incorporation and minimize compositional phase separation. Increasing the DMHy/V ratio is found to be the favored method to achieve wavelength extension. Utilization of GaAsN barrier layers instead of GaAs suppresses the spectral blue-shift of the quantum well luminescence after thermal annealing treatment. Under optimized growth conditions, InGaAsN diode lasers emitting at 1.378 μm are realized with a threshold current density of 661 A/cm^2 and external differential quantum efficiency of 34%. A slightly improved T_1 compared to our previous 1.38-μm InGaAsN–GaAs QW lasers indicates that no serious penalty exists for replacing the barrier material to a small bandgap material GaAsN. Lasing wavelengths as long as 1.41 μm with a threshold current density of 1.93 kA/cm^2 are also demonstrated, representing the *longest wavelength* InGaAsN QW lasers realized by MOCVD.

Reference

[1] D.A. Livshits, A.Y. Egorov, H. Riechert, Electron. Lett. 36 (16) (2000) 1381.

[2] M. Fischer, D. Gollub, M. Reinhardt, M. Kamp, A. Forchel, J. Crystal Growth 251 (1–4) (2003) 353.

[3] T. Takeuchi, Y.L. Chang, M. Leary, A. Tandon, H.C. Luan, D. Bour, S. Corzine, R. Twist, M. Tan, Electron. Lett. 38 (23) (2002) 1438.

[4] N. Tansu, N.J. Kirsch, L.J. Mawst, Appl. Phys. Lett. 81 (14) (2002) 2523.

[5] F. Hohnsdorf, J. Koch, S. Leu, W. Stolz, B. Borchert, M. Druminski, Electron. Lett. 35 (7) (1999) 571.

[6] M. Kawaguchi, T. Miyamoto, E. Gouardes, D. Schlenker, T. Kondo, F. Koyama, K. Iga, Jpn. J. Appl. Phys. 2—Lett. 40 (7B) (2001) L744.

[7] S. Sato, Jpn. J. Appl. Phys. 1—Regular Papers Short Notes Rev. Papers 39 (6A) (2000) 3403.

[8] P.A. Thijs, L.F. Tiemeijer, J.J.M. Binsma, T. vanDongen, IEEE J. Quantum Electron. 30 (2) (1994) 477.

[9] C.E. Zah, R. Bhat, B.N. Pathak, F. Favire, W. Lin, M.C. Wang, N.C. Andreadakis, D.M. Hwang, M.A. Koza, T.P. Lee, Z. Wang, D. Darby, D. Flanders, J.J. Hsieh, IEEE J. Quantum Electron. 30 (2) (1994) 511.

[10] D. Gollub, M. Fischer, A. Forchel, Electron. Lett. 38 (20) (2002) 1183.

[11] S.R. Bank, M.A. Wistey, H.B. Yuen, L.L. Goddard, W. Ha, J.S. Harris, Electron. Lett. 39 (20) (2003) 1445.

[12] N. Tansu, J.Y. Yeh, L. Mawst, Proceedings of the IEEE/OSA Conference on Lasers and Electro-Optics (CLEO) Paper CtuH4, Baltimore, MD, 2003.

[13] N. Tansu, J.Y. Yeh, L.J. Mawst, Appl. Phys. Lett. 83 (13) (2003) 2512.

[14] A.Y. Egorov, D. Bernklau, B. Borchert, S. Illek, D. Livshits, A. Rucki, M. Schuster, A. Kaschner, A. Hoffmann, G. Dumitras, M.C. Amann, H. Riechert, J. Crystal Growth 227 (2001) 545.

[15] T. Miyamoto, T. Kageyama, S. Makino, D. Schlenker, F. Koyama, K. Iga, J. Crystal Growth 209 (2–3) (2000) 339.

[16] F. Hohnsdorf, J. Koch, C. Agert, W. Stolz, J. Crystal Growth 195 (1–4) (1998) 391.

[17] T. Hakkarainen, J. Toivonen, M. Sopanen, H. Lipsanen, J. Crystal Growth 234 (4) (2002) 631.

[18] L.F. Bian, D.S. Jiang, S.L. Lu, J.S. Huang, K. Chang, L.H. Li, J.C. Harmand, J. Crystal Growth 250 (3–4) (2003) 339.

[19] E. Tournie, M.A. Pinault, A. Guzman, Appl. Phys. Lett. 80 (22) (2002) 4148.

[20] R. Kudrawiec, G. Sek, J. Misiewicz, D. Gollub, A. Forchel, Appl. Phys. Lett. 83 (14) (2003) 2772.

[21] V. Lordi, V. Gambin, S. Friedrich, T. Funk, T. Takizawa, K. Uno, J.S. Harris, Phys. Rev. Lett. 90 (14) (2003).

[22] P.J. Klar, H. Gruning, L. Chen, T. Hartmann, D. Golde, M. Gungerich, W. Heimbrodt, J. Koch, K. Volz, B. Kunert, T. Torunski, W. Stolz, A. Polimeni, M. Capizzi, G. Dumitras, L. Geelhaar, H. Riechert, IEE Proc.—Optoelectronics 150 (1) (2003) 28.

[23] M. Albrecht, V. Grillo, T. Remmele, H.P. Strunk, A.Y. Egorov, G. Dumitras, H. Riechert, A. Kaschner, R. Heitz, A. Hoffmann, Appl. Phys. Lett. 81 (15) (2002) 2719.

[24] H.P. Xin, K.L. Kavanagh, M. Kondow, C.W. Tu, J. Crystal Growth 202 (1999) 419.

[25] W.N. Ha, V. Gambin, S. Bank, M. Wistey, H. Yuen, S. Kim, J.S. Harris, IEEE J. Quantum Electron. 38 (9) (2002) 1260.

[26] N. Tansu, J.Y. Yeh, L. Mawst, Proceedings of the MRS Spring Meeting 2004: Symposium L: New Materials for MicroPhotonics, San Francisco, CA, USA, April 2004.